BUCKLING ANALYSIS OF LAMINATED CYLINDRICAL COMPOSITE SHELL PANEL UNDER MECHANICAL AND HYGROTHERMAL LOADS

TRAN ICH THINH, LE KIM NGOC

Hanoi University of Technology

Abstract. This paper deals with buckling of analysis multilaminated cylindrical shell panels subjected to axial and hygrothermal loadings. The geometrical non-linear analysis is carried out using the Finite Element Method based on a single layer first shear deformation theory. A nine-nodal isoparametric element with 5 degrees of freedom per node is considered. The effects of different number of layers, lamination angles, length to width ratios and hygrothermal effects are studied.

Keywords: Buckling, Composite shell panels, Hygrothermal effects, Finite Element, First-order Shear deformation Theory.

1. INTRODUCTION

Composite materials are being increasingly used in aerospace, civil, naval and other high-performance engineering application due to their light weight, high-specific strength and stiffness, excellent thermal characteristics, ease in fabrication and other significant attributes.

The effect of environment on the buckling behaviour of laminated shells and plates was studied by some authors [1], [3], [4].

In [1], Ganesan and all considered the thermal buckling in thin circular cylindrical shells using 3-nodal isoparametric element with 5 d.o.f per node. The buckling of plate and shell with higher-order displacement model, using 8-nodal serendipity element with 10 d.o.f per node are investigated by some authors [2]. Parhi and all [3] examined the hygrothermal effects on dynamic behaviour of multiple laminated composite plate and shell with large displacement model using 8-nodal element with 10 d.o.f per node. Further more, the experimental analysis in [4] showed that the rise of temperature and moisture will reduce the elastic moduli of the materials, induce internal stresses and degrade the strength of the materials. In addition, it was found that if the elastic shear modulus is much smaller than the major in-plane normal modulus, the transverse shear deformation effecting on the stability of the plate and shell will not be negligible even if these structures are not thick [5], [6].

In this paper, the 9-node isoparametric element with 5 d.o.f per node is used with Green- Lagrange strain. The effects of the number of layers, lamination angles, length to width ratios and hygrothermal are studied. In general, for the thin plate and shell panels, a good agreement is found between the obtained results and the results calculated by HSDT (Higher-order Shear Deformation Theory) [2] and by CPT (Classical Plate Theory) [7]. We can see also that hydrothermal environment has considerable effects on the buckling of the cylindrical composite shell panels.

2. FUNDAMENTAL FORMULATION

2.1. Local and global coordinate systems

Choose $OXYZ$: global coordinate system.

Choose $oxyz$: local coordinate system.

R is radius of cylindrical shell panel, L is length of straight side, b is circumferential width, h is thickness and the angle $\varphi = b/R$.

Transformation matrix between local and global axes:

$$\begin{Bmatrix} x \\ y \\ z \end{Bmatrix} = \begin{bmatrix} 1 & 0 & 0 \\ 0 & c & c \\ 0 & -s & c \end{bmatrix} \begin{Bmatrix} X \\ Y \\ Z \end{Bmatrix} \quad \text{or} \quad \begin{Bmatrix} X \\ Y \\ Z \end{Bmatrix} = \begin{bmatrix} 1 & 0 & 0 \\ 0 & c & c \\ 0 & -s & c \end{bmatrix} \begin{Bmatrix} x \\ y \\ z \end{Bmatrix},$$

with $s : \sin\varphi,\ c := \cos\varphi$

2.2. The displacement - strain fields

* *The first order displacement field* '

$$\begin{aligned} \bar{u}_{(x,y,z)} &= u^0_{(x,y)} + z\beta_{x(x,y)}, \\ \bar{v}_{(x,y,z)} &= v^0_{(x,y)} + z\beta_{y(x,y)}, \\ \bar{w}_{(x,y,z)} &= w^0_{(x,y)}, \end{aligned} \tag{2.1}$$

where, u^0, v^0, w^0 are the mid-surface displacements. β_x; β_y are the components of rotation of the normal to the reference surface in the X, Z and Y, Z - plane, respectively.

* *The strain field*

The Green-Lagrange strain model is given in the form: $\{\varepsilon\} = \{\varepsilon^l\} + \{\varepsilon^{nl}\}$, where $\{\varepsilon^l\}$ and $\{\varepsilon^{nl}\}$ represent the linear and non-linear part, respectively.

The linear part

$$\{\varepsilon^l\} = \begin{Bmatrix} \varepsilon^l_x \\ \varepsilon^l_y \\ \gamma^l_{xy} \\ \gamma^l_{yz} \\ \gamma^l_{xz} \end{Bmatrix} = \begin{Bmatrix} \varepsilon^0_x \\ \varepsilon^0_y \\ \gamma^0_{xy} \\ \gamma^0_{yz} \\ \gamma^0_{xz} \end{Bmatrix} + z \begin{Bmatrix} k_x \\ k_y \\ k_{xy} \\ 0 \\ 0 \end{Bmatrix} = \begin{Bmatrix} u^0_{,x} \\ \left(v^0_{,y} + \frac{w^0}{R}\right) \\ \left(u^0_{,y} + v^0_{,x}\right) \\ \left(\beta_y + w^0_{,y} - \frac{v^0}{R}\right) \\ \left(\beta_x + w^0_x\right) \end{Bmatrix} + z \begin{Bmatrix} \beta_{x,x} \\ \beta_{y,y} \\ (\beta_{x,y} + \beta_{y,x}) \\ 0 \\ 0 \end{Bmatrix} \tag{2.2}$$

The non-linear part

$$\{\varepsilon^{nl}\} = \begin{Bmatrix} \varepsilon^{nl}_x \\ \varepsilon^{nl}_y \\ \varepsilon^{nl}_{xy} \\ \varepsilon^{nl}_{yz} \\ \varepsilon^{nl}_{xz} \end{Bmatrix} = \begin{Bmatrix} \frac{1}{2}[\bar{u}^2_{,x} + \bar{v}^2_{,x} + \bar{w}^2_{,x}] \\ \frac{1}{2}\left[\bar{u}^2_{,y} + \left(\bar{v}_{,y} + \frac{\bar{w}}{R}\right)^2 + \left(\bar{w}_{,y} + \frac{\bar{v}}{R}\right)^2\right] \\ \left[\bar{u}_{,x}\bar{u}_{,y} + \bar{v}_{,x}\left(\bar{v}_{,y} + \frac{\bar{w}}{R}\right) + \bar{w}_{,x}\left(\bar{w}_{,y} - \frac{\bar{v}}{R}\right)\right] \\ \left[\bar{u}_{,y}\bar{u}_{,z} + \bar{v}_{,z}\left(\bar{v}_{,y} + \frac{\bar{w}}{R}\right) + \bar{w}_{,z}\left(\bar{w}_{,y} - \frac{\bar{v}}{R}\right)\right] \\ [\bar{u}_{,x}\bar{u}_{,z} + \bar{v}_{,x}\bar{v}_{,z} + \bar{w}_{,x}\bar{w}_{,z}] \end{Bmatrix} \tag{2.3}$$

2.3. Constitutive equation and hygrothermal effects

As in classical shell theory, the membrane stress resultants, the bending moment resultants and the shear stress resultants are expressed as follows:

$$\begin{Bmatrix} \{N\} \\ \{M\} \\ \{Q\} \end{Bmatrix} = \begin{bmatrix} [A] & [B] & [0] \\ [B] & [D] & [0] \\ [0] & [0] & [F] \end{bmatrix} \begin{Bmatrix} \{\varepsilon^0\} \\ \{k\} \\ \{\gamma^0\} \end{Bmatrix}. \tag{2.4}$$

The extensional, bending-stretching and bending stiffnesses of the laminated are the following:

$$[A_{ij}, B_{ij}, D_{ij}] = \int_{\frac{h}{2}}^{\frac{h}{2}} [Q'_{ij}](1, z, z^2)dz \quad \text{with} \quad (i, j = 1, 2, 3) $$

$$\text{and} \quad [F_{ij}] = \int_{\frac{h}{2}}^{\frac{h}{2}} f[Q'_{ij}]dz \quad \text{with} \quad (i, j = 4, 5). \tag{2.5}$$

"f" is the shear correction factor which is derived from the Timoshenko beam concept by applying the energy principle and is assumed as $5/6$. It accounts for the non-uniform distribution of transverse shear strain across the thickness of the lamina. "h" is the total thickness of the laminate.

The non-mechanical strains of the kth lamina due to hygrothermal effects are expressed as:

$$\begin{Bmatrix} e_x \\ e_y \\ e_{xy} \end{Bmatrix} = \begin{bmatrix} c^2 & s^2 & sc \\ s^2 & c^2 & -sc \\ -2sc & 2sc & c^2 - s^2 \end{bmatrix} \left(\begin{Bmatrix} \alpha_1 \\ \alpha_2 \\ 0 \end{Bmatrix} (T - T_0) + \begin{Bmatrix} \beta_1 \\ \beta_2 \\ 0 \end{Bmatrix} (m - m_0) \right), \tag{2.6}$$

where, c is $\cos\theta$, s is $\sin\theta$, θ_k is an arbitrary angle of fibers to ox axis; α_1, α_2, β_1, β_2 are the thermal coefficients and the moisture coefficients of lamina, respectively; m_0, T_0 are the reference moisture concentration and temperature, respectively; m, T are the elevated moisture concentration and temperature, respectively. In the present analysis, m_0 and T_0 are assumed as 0% and $27^0 C$, respectively.

The non-mechanical in plane stress and moment resultants are thus given by:

$$\{N_x^N N_y^N N_{xy}^N\}^T = \sum_{k=1}^{n} \int_{h_{k-1}}^{h_k} [Q'_{ij}]\{e\}_k dz,$$

$$\{M_x^N M_y^N M_{xy}^N\}^T = \sum_{k=1}^{n} \int_{h_{k-1}}^{h_k} [Q'_{ij}]\{e\}_k z dz \quad \text{with} \quad (i, j = 1, 2, 6). \tag{2.7}$$

3. FINITE ELEMENT PROCEDURE

In numerical analysis by the F.E.M, the element model we choose is a nine-nodal isoparametric element with 5 d.o.f considered at each node of the element that are u, v, w, β_x and β_y. Where, β_x and β_y are the components of rotation of the normal to the reference surface in the X, Z and Y, Z - plane, respectively. The displacement field and geometrical parameters are thus given as:

$$u = \sum_{i=1}^{9} N_i u_i; \quad v = \sum_{i=1}^{9} N_i v_i; \quad w = \sum_{i=1}^{9} N_i w_i;$$

$$\beta_x = \sum_{i=1}^{9} N_i \beta_{xi}; \quad \beta_y = \sum_{i=1}^{9} N \beta_{yi};$$

$$x = \sum_{i=1}^{9} N_i x_i; \quad y = \sum_{i=1}^{9} N_i y_i;$$

The interpolation functions N_i are given as [10]:

$$N_1 = \tfrac{1}{4}(1-\xi)(1-\eta)\xi\eta; \quad N_4 = \tfrac{1}{2}(1+\xi)(1-\eta^2)\xi; \quad N_7 = -\tfrac{1}{4}(1-\xi)(1+\eta)\xi\eta;$$

$$N_2 = -\tfrac{1}{2}(1-\xi^2)(1-\eta)\eta; \quad N_5 = \tfrac{1}{4}(1+\xi)(1+\eta)\xi\eta; \quad N_8 = -\tfrac{1}{2}(1-\xi)(1-\eta^2)\xi;$$

$$N_3 = -\tfrac{1}{4}(1+\xi)(1-\eta)\xi\eta; \quad N_6 = \tfrac{1}{2}(1-\xi^2)(1+\eta)\eta; \quad N_9 = (1-\xi^2)(1-\eta^2).$$

The stiffness matrix of element is given by:

$$[K_e] = \int_{-1}^{1}\int_{-1}^{1} \begin{bmatrix} [N_i]^T[L_1]^T[A][L_1][N_i] + [N_i]^T[L_1]^T[B][L_2][N_i] \\ +[N_i]^T[L_2]^T[B][L_1][N_i] + [N_i]^T[L_2]^T[D][L_2][N_i] \\ +[N_i]^T[L_3]^T[F][L_3][N_i] \end{bmatrix} |J| d\xi d\eta, \qquad (3.1)$$

where, **J** is the Jacobian matrix; $[L_i]$ are usual strain-displacement operator matrix.

Putting (2.1) into (2.3), the non-linear strains are modified. And then, the $\{\varepsilon^{nl}\}$ are expressed in matrix form as $\{\varepsilon^{nl}\} = \{\varepsilon_x^{nl} \varepsilon_y^{nl} \varepsilon_{xy}^{nl} \varepsilon_{xz}^{nl} \varepsilon_{yz}^{nl}\}^T = \tfrac{1}{2}[\Omega]_{5\times 9}\{\delta_e\}_{9\times 1}$, where, $[\Omega]$ is the multiplier matrix (appendix) and:

$$\{\delta_e\} = \Big\{ (u_{,x}^0 + z\beta_{x,x}), (v_{,x}^0 + z\beta_{y,x}), w_{,x}^0, (u_{,y}^0 + z\beta_{x,y}), \Big((v_{,y}^0 + \frac{w^0}{R}) + z\beta_{y,y}\Big),$$

$$\Big(w_{,y}^0 + \big(-\frac{v^0}{R}\big)\Big), \beta_x, \beta_y, 0 \Big\}^T.$$

This vector can be expressed in the form of nodal degree of freedom: $\{\delta_e\}_{9\times 1} = [G]_{9\times 45}\{q_e\}_{45\times 1}$, where, $\{q_e\} = \{u_1 \, v_1 \, w_1 \, \beta_{x1} \, \beta_{y1}...\beta_{x9} \, \beta_{y9}\}_{45\times 1}^T$ is the element displacement vector, $[G]$ is the initial strain-displacement operator matrix.

The strain energy is determined by initial stresses in the form [3] as well as [8]:

$$[U_e^{\sigma,N}] = \frac{1}{2} \int\limits_{V_e} \{\delta_e\}^T \begin{bmatrix} S_e & 0 & 0 \\ 0 & S_e & 0 \\ 0 & 0 & S_e \end{bmatrix} \{\delta_e\} dV, \tag{3.2}$$

where,

$$[S_e]_{3\times 3} = \begin{bmatrix} \sigma_x^i & \tau_{xy}^i & \tau_{xz}^i \\ & \sigma_y^i & \tau_{yz}^i \\ (Sym) & & 0 \end{bmatrix};$$

superscript $(^i)$ represents corresponding initial stresses.

So, the initial stress (or geometric) stiffness matrices of element are expressed by:

$$K_e^{\sigma,N} = \int\limits_{V_e} [G]^T \begin{bmatrix} S_e & 0 & 0 \\ 0 & S_e & 0 \\ 0 & 0 & S_e \end{bmatrix} [G] dV. \tag{3.3}$$

After some calculations, we obtain:

$$[K_e^{\sigma,N}] = [K_{e1}^{\sigma,N}] + [K_{e2}^{\sigma,N}] + [K_{e3}^{\sigma,N}] + [K_{e4}^{\sigma,N}], \tag{3.4}$$

where,

$$[K_{e1}^{\sigma,N}] = \int\limits_{-1}^{1}\int\limits_{-1}^{1} [N_i]^T [L_1^\sigma]^T \begin{bmatrix} S_{e1} & 0 & 0 \\ 0 & S_{e1} & 0 \\ 0 & 0 & S_{e1} \end{bmatrix} [L_1^\sigma][N_i]|J|d\xi d\eta,$$

$$[K_{e2}^{\sigma,N}] = \int\limits_{-1}^{1}\int\limits_{-1}^{1} [N_i]^T [L_2^\sigma]^T \begin{bmatrix} S_{e2} & 0 & 0 \\ 0 & S_{e2} & 0 \\ 0 & 0 & S_{e2} \end{bmatrix} [L_1^\sigma][N_i]|J|d\xi d\eta,$$

$$[K_{e3}^{\sigma,N}] = \int\limits_{-1}^{1}\int\limits_{-1}^{1} [N_i]^T [L_1^\sigma]^T \begin{bmatrix} S_{e3} & 0 & 0 \\ 0 & S_{e3} & 0 \\ 0 & 0 & S_{e3} \end{bmatrix} [L_2^\sigma][N_i]|J|d\xi d\eta,$$

$$[K_{e4}^{\sigma,N}] = \int\limits_{-1}^{1}\int\limits_{-1}^{1} [N_i]^T [L_2^\sigma]^T \begin{bmatrix} S_{e4} & 0 & 0 \\ 0 & S_{e4} & 0 \\ 0 & 0 & S_{e4} \end{bmatrix} [L_2^\sigma][N_i]|J|d\xi d\eta,$$

with

$$[S_{e1}]_{3\times3} = \begin{bmatrix} N_x & N_{xy} & Q_x \\ & N_y & Q_y \\ (Sym) & & 0 \end{bmatrix},$$

$$[S_{e2}]_{3\times3} = [S_{e3}]_{3\times3} = \begin{bmatrix} M_x & M_{xy} & Q_x^* \\ & M_y & Q_y^* \\ (Sym) & & 0 \end{bmatrix},$$

$$[S_{e4}]_{3\times3} = \begin{bmatrix} M_x^* & M_{xy}^* & Q_x^{**} \\ & M_y^* y & Q_y^{**} \\ (Sym) & & 0 \end{bmatrix},$$

in which, superscript (*) and (**) represent corresponding the higher-order force resultants.

The transformation matrix, $[T]$, from local to global axes is in the form:

$$[T]_{9\times9} = \begin{bmatrix} [t_i] & 0 & K & 0 \\ & [t_i] & & \\ & & 0 & M \\ (Sym) & & & [t_i] \end{bmatrix} \text{ with } [t_i] = \begin{bmatrix} 1 & 0 & 0 & 0 & 0 \\ 0 & c & -s & 0 & 0 \\ 0 & s & c & 0 & 0 \\ 0 & 0 & 0 & 1 & 0 \\ 0 & 0 & 0 & 0 & c \end{bmatrix}_{(5\times5)}. \quad (3.5)$$

Finally, the buckling problem is reduced to the eigenvalue problem:

$$([\mathbf{K}] + [\mathbf{K^N}] - \lambda[\mathbf{K}^\sigma]\{\mathbf{Q}\} = \mathbf{0}. \quad (3.6)$$

In order to solve this eigenvalue problem, the Subspace Iteration Method is applied [14]. The least eigenvalue λ corresponds to the buckling load of the shell panel will be obtained.

Note that the mechanical load is an uniform-axial compressive load on curved edges. The (3×3) Gauss quadrature is used to calculate the integral expressions.

The element nodal load vector due to hygrothermal effects is determined by

$$[\mathbf{P_e^N}] = \int\limits_{S_e} [\mathbf{B}]^T\{\mathbf{F}^N\}ds, \quad (3.7)$$

where, $\{\mathbf{F^N}\} = \{N_x^N N_y^N N_{xy}^N M_x^N M_y^N M_{xy}^N 00\}$ as mentioned earlier in (2.7) and $[B] = [L][N_i]$ is the strain-displacement matrix.

The solution procedure for the buckling problem includes the following steps:

- From (3.1), one can compute the stiffness matrix $[K]$ by assembling the element stiffness matrices.

- Solution of the prebuckling problem to determined the stress resultants due to the mechanical load:

$$[\mathbf{K}]\{\mathbf{Q}\} = \{\mathbf{P}\}, \tag{3.8}$$

where, $\{\mathbf{Q}\}$ is the global displacement vector.

- Compution of the prebuckling geometric stiffness matrix, $[\mathbf{K}^\sigma]$.

- Solution of the hygrothermal problem to obtain the stress resultants due to the temperature change and moisture concentration:

$$[\mathbf{K}]\{\mathbf{Q}\} = \{\mathbf{P^N}\}. \tag{3.9}$$

- Computation of the initial stress (or geometric) stiffness matrix, $[\mathbf{K^N}]$.

- Determination of the buckling load from (3.6).

4. NUMERICAL RESULTS AND DISCUSSION

In order to bring out numerical solutions of the buckling problem with and without hygrothermal effects for a cylindrical composite shell panel, in this section, some kinds of composite shell panels were calculated by the Matlab software (a mesh of 4×4 elements for a full shell panel).

Geometrical parameters are as in Fig. 1.

- Length of straight side: L
- Circumferential width: b
- Thickness: h
- Radius of cylindrical shell panel: R
- $\varphi = \frac{b}{R}$
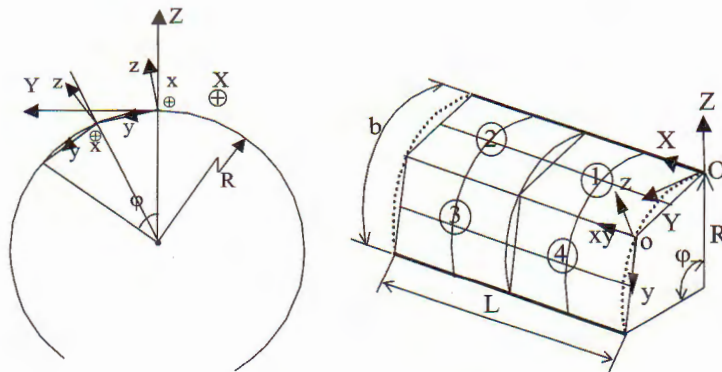
Fig. 1. Geometrical parameter

4.1. The buckling parameter of cylindrical panels subjected to axial compression

A symmetric lay-up $[0/-\theta^0/\theta^0/90^0]_s$, θ: fibre angle ranging from $0^0 - 90^0$ with steps of 15^0 is analyzed.

The material and geometrical properties are: $E_1 = 181\,\text{GPa}$; $E_2 = 10.3\,\text{GPa}$; $G_{12} = G_{13} = G_{23} = 7.17\,\text{GPa}$; $\nu_{12} = \nu_{13} = \nu_{23} = 0.28$; $h = 1\text{mm}$; $R/h = 150$; $L/R = 1$ and $b/L = 1.309, 1.047$ and 0.786.

Boundary conditions are imposed as in Table 1 (note: 0 - free to move, 1- fixed).

The uniaxial non-dimensionalized buckling parameter $\lambda = F_{cr}R/E_1h^2$ versus lamination angle fibre θ^0 for a thin cylindrical panel ($R/h =150$) is presented in Table 2 and Fig. 2 - 4.

Table 1. Boundary conditions

	u	v	w	β_x	β_y
Top	0	1	1	1	0
Right side	0	1	1	1	1
Bottom	0	1	1	1	0
Left side	1	1	1	1	1

Table 2. Effects of angle fibre on buckling load parameter λ ($R/h = 150$)

θ^0	$\lambda = F_{cr}R/E_1h_2$								
	$b/L = 1.309$			$b/L = 1.047$			$b/L = 0.786$		
	CPT[7]	HSDT[2]	Present	CPT[7]	HSDT[2]	Present	CPT[7]	HSDT[2]	Present
0	0.117	0.121	0.118	0.123	0.122	0.119	0.126	0.129	0.129
15	0.170	0.147	0.149	0.147	0.147	0.151	0.155	0.159	0.156
30	0.197	0.190	0.187	0.194	0.192	0.188	0.202	0.205	0.202
45	0.221	0.211	0.215	0.222	0.220	0 0.217	0.230	0.232	0.233
60	0.212	0.206	0.208	0.214	0.214	0.212	0.225	0.230	0.227
75	0.171	0.174	0.175	0.174	0.179	0.177	0.187	0.193	0.192
90	0.142	0.147	0.151	0.144	0.155	0.155	0.155	0.163	0.160

From the Table 2 and Fig. 2 - 4, we see that a good agreement is found between the present results, the numerical predictions of the HSDT and the numerical predictions of the CPT. Fibre angle influences considerably on the stability of the cylindrical shell panel. The $[0/ - 45^o/45^o/90^o]_s$ is the most stable; the $[0^o/0^o/0^o/90^o]_s$ is the least stable. The difference of λ (between the $[0/ - 45^o/45^o/90^o]_s$ and the $[0^o/0^o/0^o/90^o]_s$ shell panel) is about 45% when $b/L = 1.309$, about 44% when $b/L = 1.047$ and about 45% when $b/L = 0.786$.
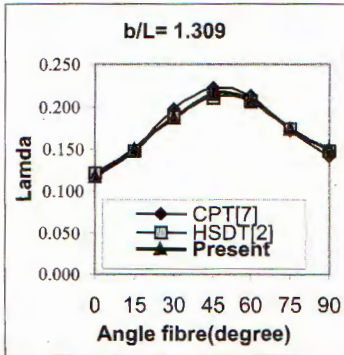

Fig. 2. Effects of angle fibre on buckling load parameter λ with b/L=1.309; R/h=150
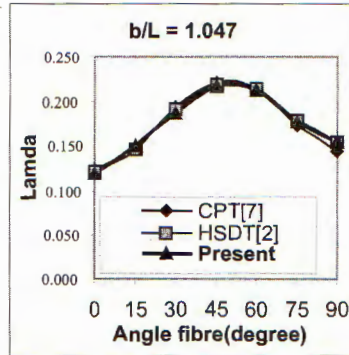
Fig. 3. Effects of angle fibre on buckling load parameter λ with b/L=1.047; R/h=150

Fig. 4. Effects of angle fibre on buckling load parameter λ with b/L=0.786; R/h=150

The uniaxial non-dimensionalized buckling parameter $\lambda = F_{cr}R/E_1h^2$ versus lamination angle fibre θ^0 for a thick cylindrical panel $(R/h = 15)$ is presented in Fig. 5 - 7.
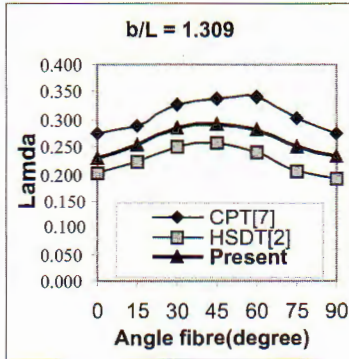

Fig. 5. Effects of angle fibre on buckling load parameter with b/L=1.309; R/h=15
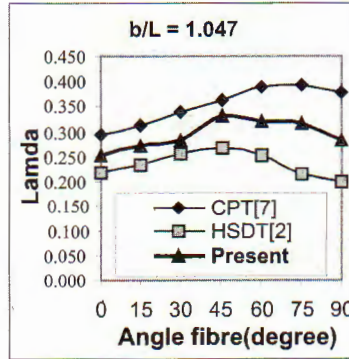
Fig.6. Effects of angle fibre on buckling load parameter with b/L=1.047; R/h=15
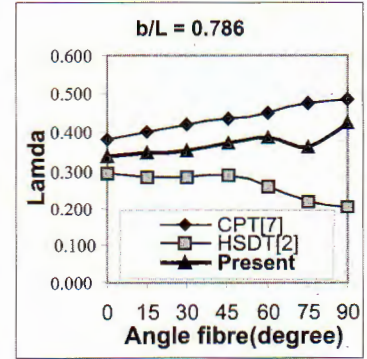
Fig. 7. Effects of angle fibre on buckling load parameter with b/L=0.786; R/h=15

From the Fig. 5 - 7, we see that the difference of the numerical results between Present and CPT models ranges from about 10% to 31%; between Present and HSDT models ranges from about 11%

4.2. Buckling load parameter of composite plates $(R = \infty)$ subjected to axial compression

The antisymmetric lay-up $[\theta^0/ - \theta^0/...]_{-s}$, θ^0: fibre angle ranging from $0^0 - 90^0$ with steps of 15^0 is analyzed.

The material and geometrical properties are: $E_2 = 6.9\,\text{GPa}$; $E_1/E_2 = 40\,\text{GPa}$; $G_{12} = G_{13} = G_{23} = 3.45\,\text{GPa}$; $\nu_{12} = \nu_{13} = \nu_{23} = 0.25$; $h = 5\,\text{mm}$; $L/h = 100$; $L/a = 1$.
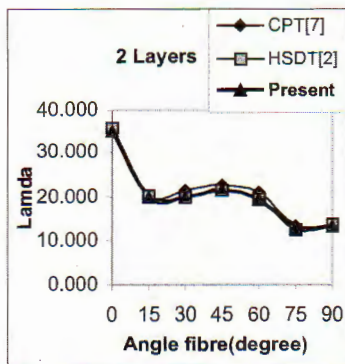
Fig. 8. Effect of number of layers and angle fibre on buckling load parameter λ, 2 layers
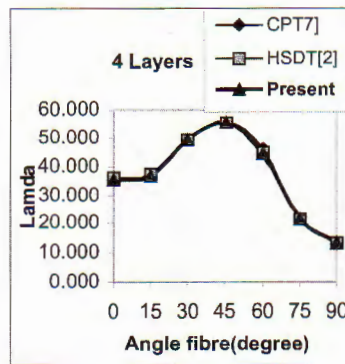
Fig. 9. Effect of number of layers and angle fibre on buckling load parameter λ, 4 layers
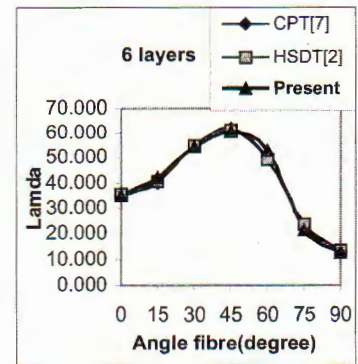
Fig. 10. Effect of number of layers and angle fibre on buckling load parameter λ, 6 layers

Boundary conditions are imposed as in table 3. The effect of number of layer on the non-dimensional buckling parameter $\lambda = F_{cr}a^2/E_2h^3$ for an antisymmetric thin laminated square plate (a/h =100) are presented in Fig. 8 - 10.

From the Fig. 8 - 10 we see that a good agreement is observed for thin plate between the proposed model and the alternative solutions. It is possible to say that the mathematical model is reasonable.

Table 3. Boundary conditions

	u	v	w	β_x	β_y
Top	0	0	1	1	0
Right side	0	0	1	0	1
Bottom	0	1	1	1	0
Left side	1	0	1	0	1

4.3. Hygrothermal effects on the buckling of laminated cylindrical composite shell panel

Assume that the change of temperature is constant in each layer. T_0: 27^0C; $T : 27^0C$ and 152^0C thus, ΔT: 0^0C and 125^0C and the change of moisture concentration is constant from the external layer to internal one with $\Delta m_s = 1.5\%$.(the shell panel was almost saturated).

The symmetric lay-up $[0/ - \theta^0/\theta^0/90^0]_s$, θ^0: fibre angle ranging from $0^0 - 90^0$ with steps of 15^0 is analyzed. The material and geometrical properties are: $E_1 = 181$ GPa; E_2= 10.3 GPa; $G_{12} = G_{13} = G_{23} = 7.17$ GPa; $\nu_{12} = \nu_{13} = \nu_{23} = 0.28$; $h = 1$ mm; $R/h = 150$; $L/R = 1$ and $b/L = 1.309, 1.047$ and 0.786. Boundary conditions are as in Table 1 .

The non-dimensionalized buckling load parameters $\lambda = (F_{cr}^N.R/E_1.h^2)$ when the thin shell panel subjected to temperature and moisture simultaneously are as in the Table 4 and Fig. 11-13. (superscript $(^N)$ represents corresponding non-mechanical load).

Table 4. Hygrothermal effects and angle fibre on buckling load parameter λ

θ^0	$\lambda = F_{cr}R/E_1h^2$								
	$b/L = 1.309$			$b/L = 1.047$			$b/L=0.786$		
	Present		(III)	Present		(III)	Present		(III)
	(I)	(II)		(I)	(II)		(I)	(II)	
0	0.120	0.098	18.1%	0.119	0.098	17.5%	0.129	0.108	16.3%
15	0.154	0.119	22.6%	0.151	0.118	21.7%	0.156	0.124	20.7%
30	0.192	0.139	27.7%	0.187	0.137	26.5%	0.202	0 0.150	25.5%
45	0.215	0.150	30.2%	0.217	0.153	29.4%	0.233	0.167	28.4%
60	0.208	0.146	29.9%	0.212	0.151	28.9%	0.227	0.164	27.9%
75	0.175	0.133	24.2%	0.177	0.135	23.9%	0.192	0.148	22.9%
90	0.151	0.132	12.4%	0.155	0.136	11.9%	0.160	0.143	10.9%

(I) without hygrothermal;(II) with hygrothermal; (III) Discrepancy.

From the Tables 4 and Fig. 11 - 13, we see that the environment has considerable effects on the buckling load parameter (λ) of the cylindrical composite shell panel. The reductions

of the λ for the $[0/-\theta^0/\theta^0/90^0]_s$ shell panel range from about 10% to 30%. When subjected to the hygrothermal effects, the λ for the $[0/90^0/90^0/90^0]_s$ shell panel is least degraded (about 10%); the λ for the $[0/-45^0/45^0/90^0]_s$ shell panel is most degraded (about 30%), although this configuration is the most stable in the case of without hygrothermal load.
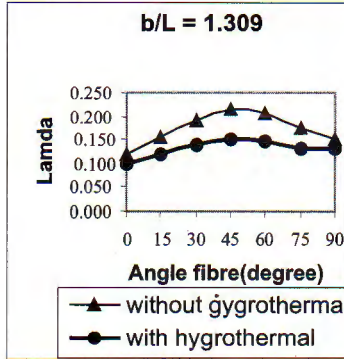

Fig. 11. Hygrothermal effects and angle fibre on buckling load parameter with b/L=1.309
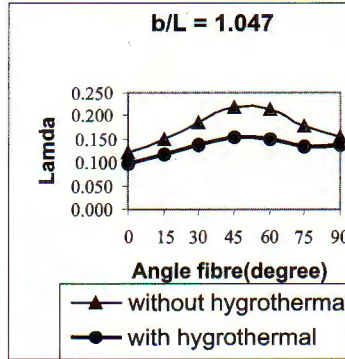
Fig. 12. Hygrothermal effects and angle fibre on buckling load parameter λ with b/L=1.047
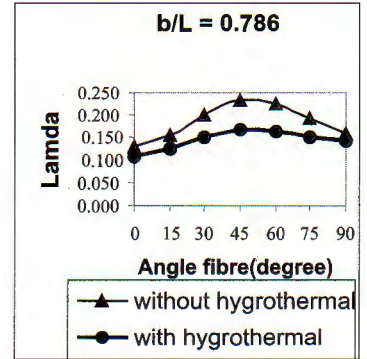
Fig. 13. Hygrothermal effects and angle fibre on buckling load parameter with b/L=0.786

5. CONCLUSION

The single layer first shear deformation with Green-Lagrange strain model was applied in modeling the buckling behaviour of composite shell panels. In the Finite Element Procedure, the 9-nodal isoparametric element with 5 degrees of freedom per node was chosen. The following broad conclusions may be made from the results presented in the earlier section:

1. For the thin plate and shell panels, the present results obtained by using a full panel 4×4 finite element mesh are good argreement with existing solutions (CPT and HSDT). The present model gives, relatively speaking, faster convergent solution when compared to the HSDT model (10×10 mesh).

2. For the thick plate and shell panels, CPT overpredicts the buckling loads; HSDT underpredicts the buckling loads and the present model gives the intermediate values of buckling loads when the number of layer is increased. It can be noted that the transverse shear deformation has effect on the buckling loads of the composite shell panels.

3. Concerning the hygrothermal effects, one can see the considerable influence on the buckling parameters of the shell panels. For example, the buckling parameter for the $[0/-45^0/45^0/90^0]_s$ is degraded until 30% (when $\Delta m_s = 1.5\%$ and $\Delta T = 125^0$C).

From all obtained results, it is necessary to pay attention to the effects of the number of layers, lamination angles, length to width ratios, especially, effects of temperature and moisture in design as well as in studying the static or dynamic behaviour of laminated composite shells.

REFERENCES

1. N. Ganesan, Ravikiran Kadoli, Buckling and dynamic analysis of thermopiezoelectric composite cylindrical shell, *Composite and Structures* **59** (2003) 45-60.

2. Jos Simes Moita, Cristvo M. Mota Soares, Carlos A.Mota Soares, Buckling and dynamic behavior of laminated composite structures using a discrete higher-order displacement model, *Computers and Structures* **73** (1999) 407-423.

3. P. K. Parhi, S. K. Bhattacharyya, P. K. Sinha, Hygrothermal effects on the dynamic behavior of multi laminated composite plates and shells, *Journal of Sound and Vibration* **248** (2) (2001) 195-214.

4. C. H. Shen and G. S. Springer , Moisture absorption and desorption of composite material, *J. comp. Mater.* **10** (1976) 2-20.

5. G. A. Cohen , Effect of transverse shear deformation on anisotropic plate buckling, *J. comp. Mater.* **16** (1982) 301-312.

6. N. D. Phan and J. N. Reddy, Analysis of laminated composite plates using a high-order shear deformation theory, *Int. J. Numer. Math. Engine* **21** 2201-2219.

7. J. S. Moita , C. M. Mota Soares ,C. A. Mota Soares ., Vibration and buckling of thin laminated composite structures, *Education, Practice and Promotion of Computational Methods in Engineering Using Small Computers,* **2** (1995) 263-1269, Korea. Korea Techno.

8. O. C. Zienkievicz, *The Finite Element Method in Engineering Science*, Maidenhead, Mc.Graw-Hill Publishing Co.Ltd, 1975.

9. Trần Ích Thịnh, *Vật Liệu Composite - Cơ Học và Tính Toán Kết Cấu*, Nxb Giáo dục , Hà Nội, 1994.

10. Chu Quốc Thắng, *Phương pháp phần tử hữu hạn*, Nxb Khoa học và kỹ thuật, 1997.

11. S. Ahmad, B. M. Irons and O. C. Zienkiewicz, Analysis of thick and thin shell structures by curved element, *Int. J. Numer. Math. Engine* **2** (1970) 419-453.

12. H. Parisch,A critical survey of the 9-node degenerated shell element with special emphasis on thin shell application and reduced integration, *Comp. Math. appl. Mech. Engine* **20** (1979) 323-350.

13. K. Stolarski and T. Belytschko, Shear and membrane locking in curved Co element, *Comp. Math. appl. Mech. Engine* **41** (1983) 279-296.

14. Klaus-Jurgen Bathe, *Finite Element Procedures*, pp.954-965.

PHÂN TÍCH ỔN ĐỊNH MẢNH VỎ TRỤ COMPOSITE LỚP DƯỚI TÁC DỤNG CỦA TẢI TRỌNG CƠ HỌC VÀ NHIỆT- ẨM

Báo cáo tập trung nghiên cứu ổn định đàn hồi mảnh vỏ trụ composite lớp chịu tác dụng của lực nén dọc trục trong môi trường nhiệt-ẩm. Phân tích được thực hiện nhờ Phần tử hữu hạn tứ giác 9 nút dựa vào lý thuyết biến dạng bậc nhất, có tính đến yếu tố phi tuyến hình học. Ảnh hưởng của số lớp vật liệu, góc đặt cốt, tỉ số chiều dài/chiều rộng và của yếu tố nhiệt- ẩm đã được khảo sát.